SEMI-SUPERVISED SEMANTIC SEGMENTATION NEEDS STRONG, HIGH-DIMENSIONAL PERTURBATIONS

Anonymous authors
Paper under double-blind review

ABSTRACT

Consistency regularization describes a class of approaches that have yielded ground breaking results in semi-supervised classification problems. Prior work has established the cluster assumption — under which the data distribution consists of uniform class clusters of samples separated by low density regions — as key to its success. We analyze the problem of semantic segmentation and find that the data distribution does not exhibit low density regions separating classes and offer this as an explanation for why semi-supervised segmentation is a challenging problem. We then identify the conditions that allow consistency regularization to work even without such low-density regions. This allows us to generalize the recently proposed CutMix augmentation technique to a powerful masked variant, CowMix, leading to a successful application of consistency regularization in the semi-supervised semantic segmentation setting and reaching state-of-the-art results in several standard datasets.

1 INTRODUCTION

Semi-supervised learning offers the tantalizing promise of training a machine learning model with limited amounts of labelled training data and large quantities of unlabelled data. These situations often arise in practical computer vision problems where large quantities of images are readily available and generating ground truth labels acts as a bottleneck due to the cost and labour required.

Consistency regularization (Sajjadi et al., 2016b; Laine & Aila, 2017; Miyato et al., 2017; Oliver et al., 2018) describes a class of semi-supervised learning algorithms that have yielded state-of-the-art results in semi-supervised classification, while being conceptually simple and often easy to implement. The key idea is to encourage the network to give consistent predictions for unlabeled inputs that are perturbed in various ways.

The effectiveness of consistency regularization is often attributed to the *smoothness assumption* (Miyato et al., 2017; Luo et al., 2018) or *cluster assumption* (Chapelle & Zien, 2005; Sajjadi et al., 2016a; Shu et al., 2018; Verma et al., 2019). The smoothness assumption states that samples close to each other are likely to have the same label. The cluster assumption — a special case of the smoothness assumption — states that decision surfaces should lie in low density regions, not crossing high density regions. This typically holds in classification tasks, where most successes of consistency regularization have been reported so far.

On a high level, semantic segmentation is classification, where each pixel is classified based on its neighborhood. It is therefore intriguing that consistency regularization has not been clearly beneficial in this context. We make the observation that the distance between patches centered on neighboring pixels varies smoothly even when the class of the center pixel changes, and thus there are no low-density regions on class boundaries. This alarming observation leads us to investigate the conditions that can allow consistency regularization to operate even in these conditions. Our key insight is that this is indeed possible, and that previous attempts have yielded little success primarily because the perturbations they used were not strong enough, and especially not high-dimensional enough.

We show that a flexibly masked variant of CutMix (Yun et al., 2019), which we call CowMix based on the mask appearance, does realize significant gains in semi-supervised semantic segmentation. This result clearly signposts a direction where further improvements are likely to be available.

2 BACKGROUND

Our work relates to prior art in three areas: recent regularization techniques for classification, semi-supervised classification with a focus on consistency regularization, and semantic segmentation.

2.1 MIXUP, CUTOUT, AND CUTMIX

The MixUp regularizer of Zhang et al. (2018) improves the performance of supervised image, speech and tabular data classifiers by using interpolated samples during training. The inputs and target labels of two randomly chosen examples are blended using the same randomly chosen factor.

The Cutout regularizer of DeVries & Taylor (2017) augments an image by masking a rectangular region to zero. The recently proposed CutMix regularizer of Yun et al. (2019) combines aspects of MixUp and Cutout, cutting a rectangular region from B and pasting it over A. MixUp, Cutout, and CutMix improve supervised classification performance, with CutMix outperforming the other two.

2.2 SEMI-SUPERVISED CLASSIFICATION

The Π-model of Laine & Aila (2017) passes each unlabeled sample through a classifier twice, applying two realizations of a stochastic perturbation process, and minimizes the difference between the resulting class probability predictions. Their temporal model maintains a per-sample moving average of historical predictions and encourages subsequent predictions to be consistent with the average. Sajjadi et al. (2016b) similarly encourage consistency between the current and historical predictions. Miyato et al. (2017) improve the results by replacing the stochastic perturbations with adversarial directions, thus focusing on perturbations that are closer to the decision boundaries.

The mean teacher model of Tarvainen & Valpola (2017) encourages consistency between predictions of a student network and a teacher network. The teacher's weights are an exponential moving average (Polyak & Juditsky, 1992) of those of the student, leading to a faster convergence and improved results. French et al. (2018) adapt the mean teacher approach for domain adaptation.

Interpolation consistency training (ICT) (Verma et al., 2019) and MixMatch (Berthelot et al., 2019) both combine MixUp (Zhang et al., 2018) with consistency regularization. ICT uses the mean teacher model and applies MixUp to unsupervised samples, blending input images along with teacher class predictions to produce a blended input and target to train the student. MixMatch stochastically perturbs each sample multiple times and averages the predictions to produce unsupervised targets; MixUp is applied to labeled as well as unlabeled samples.

2.3 SEMANTIC SEGMENTATION

Long et al. (2015) finetune a pre-trained VGG-16 (Simonyan & Zisserman, 2014) image classifier to produce a dense set of predictions for overlapping input windows. They effectively transform the image classifier into a fully convolutional network that can be used to segment input images of arbitrary size. Various methods were proposed for increasing the localization accuracy of the results (Long et al., 2015; Chen et al., 2014; Mostajabi et al., 2014) until the introduction of encoder-decoder networks (Badrinarayanan et al., 2015; Ronneberger et al., 2015) led to a solution where the output resolution natively matches the input. In these recent methods the encoder downsamples the input progressively, similarly to image classifiers, the decoder performs progressive upsampling, and skip connections route data between the matching resolutions of the two networks, improving the ability to accurately segment fine details.

A number of approaches for semi-supervised semantic segmentation use additional data. Kalluri et al. (2018) use data from two datasets from different domains, maximizing the similarity between per-class embeddings from each dataset. Stekovic et al. (2018) use depth images and enforced geometric constraints between multiple views of a 3D scene. Relatively few approaches operate in a strictly semi-supervised setting. Hung et al. (2018) employ adversarial learning, using a discriminator network that distinguishes real from predicted segmentation maps to guide learning. Perone & Cohen-Adad (2018) apply consistency regularization to a MRI volume dataset and their method is the only successful application of consistency regularization to segmentation that we are aware of.

(a) Example image | (b) Avg. distance to neighbor, patch size 15×15 | (c) Avg. distance to neighbor, patch size 225×225
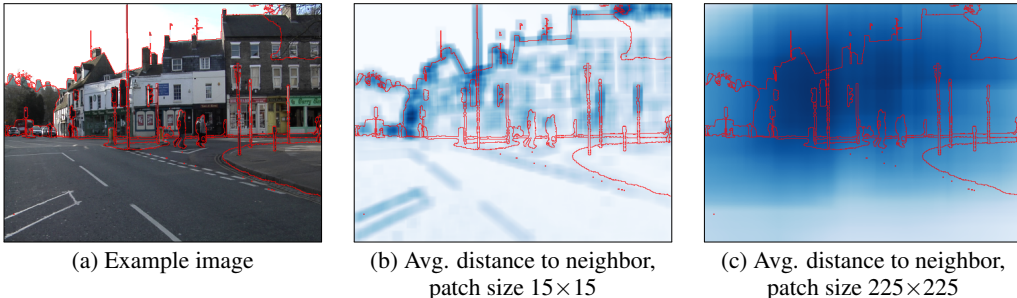
Figure 1: In a segmentation task, low-density regions rarely correspond to class boundaries. (a) An image from Camvid dataset. (b) Average L^2 distance between a patch centered at pixel and its four immediate neighbors, using 15×15 pixel patches. (c) Same for a more realistic receptive field size of 225×225 pixels. Dark blue indicates large inter-patch distance and therefore a low density region, white indicates a distance of 0. The red lines indicate segmentation ground truth boundaries.

3 CONSISTENCY REGULARIZATION FOR SEMANTIC SEGMENTATION

Consistency regularization adds a consistency loss term L_{cons} to the loss that is minimized during training (Oliver et al., 2018). In a classification task, L_{cons} measures a distance $d(\cdot, \cdot)$ between the predictions resulting from applying a neural network f_θ to an unsupervised sample x and a perturbed version $\hat{x}$ of the same sample, i.e., $L_{cons} = d(f_\theta(x), f_\theta(\hat{x}))$. The perturbation used to generate $\hat{x}$ depends on the variant of consistency regularization used. A variety of distance measures $d(\cdot, \cdot)$ have been used, e.g., squared distance (Laine & Aila, 2017) or cross-entropy (Miyato et al., 2017).

Athiwaratkun et al. (2019) analyze a simplified version of the Π-model (Laine & Aila, 2017) in which perturbation consists of additive Gaussian noise so that $\hat{x} = x + \epsilon h$, where $h \sim \mathcal{N}(0, I)$ and $d(\cdot, \cdot)$ is a squared Euclidean distance. For small constant ϵ, the expected value of the consistency loss term L_{cons} is approximately proportional to the square of the Frobenius norm of the Jacobian $J_{f_\theta}(x)$ of the networks outputs with respect to its inputs:

$$\mathbb{E}[L_{cons}] = \mathbb{E}\left[\left\|f_\theta(x + \epsilon h) - f_\theta(x)\right\|^2\right] \approx \epsilon^2 \left\|J_{f_\theta}(x)\right\|_F^2. \tag{1}$$

Thus, minimizing L_{cons} directly flattens the decision function in the vicinity of unsupervised samples. This illustrates clearly the mechanism by which consistency regularization encourages the network to move the decision boundary — and its surrounding region of high gradient — into regions of low sample density.

3.1 WHY SEMI-SUPERVISED SEMANTIC SEGMENTATION IS CHALLENGING

We attribute the infrequent success of consistency regularization in semantic segmentation problems to the observation that low density regions in input data do not align well with class boundaries. As illustrated in Figure 1, the cluster assumption is clearly violated: how much the contents of the receptive field of one pixel differ from the contents of the receptive field of a neighboring pixel has effectively no correlation with whether the patches' center pixels belong to the same class or not. For the cluster assumption to hold, we would require the distances between the contents of receptive fields to be large between classes and small within classes, which is not the case here.

The lack of variation in the patchwise distances is easy to explain from a signal processing perspective. With patch shape B, the L^2 distance between two patches centered at, say, horizontally neighboring pixels can be written as $\sqrt{B * (\Delta_x x)^2}$, where $*$ denotes convolution and $\Delta_x x$ is the horizontal gradient of the input image x. The squared gradient image is thus low-pass filtered by a B-shaped box filter, which suppresses any fine details and leads to smoothly varying sample density across the image.
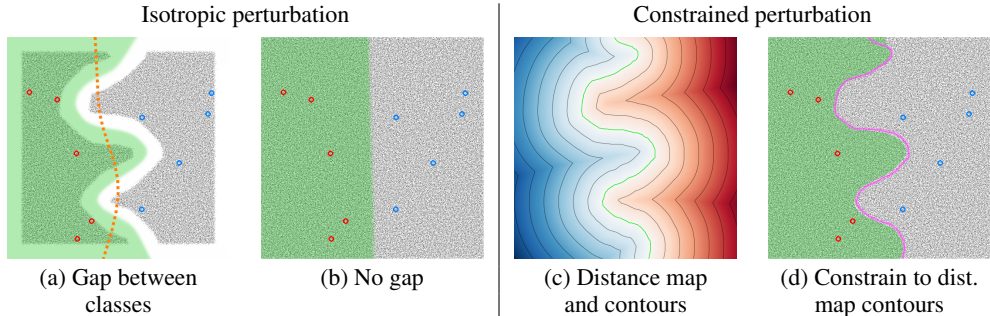
3

Figure 2: 2D semi-supervised classification experiments. Blue and red circles indicate supervised samples from class 0 and 1 respectively. The field of small black dots indicate unsupervised samples. The learned decision function is visualized by rendering the probability of class 1 in green; the soft gradation represents the gradual change in predicted class probability. (a, b) Semi-supervised learning with and without a low density region separating the classes. The dotted orange line in (a) shows the decision boundary obtained with plain supervised learning. (c) Rendering of the distance to the true class boundary with distance map contours. (d) Decision boundary learned when samples are perturbed along distance contours. The magenta line indicates the true class boundary. Appendix A explains the setup in detail.

3.2 CONSISTENCY REGULARIZATION WITHOUT CLUSTER ASSUMPTION

Let us analyze a simple toy example of learning to classify 2D points in a semi-supervised fashion. Figure 2a illustrates the setup where cluster assumption holds and there is a gap between the unsupervised samples belonging to the two different classes. The perturbation used for the consistency loss is a simple Gaussian nudge to both coordinates, and as expected, the learned decision boundary settles neatly between the two clusters.

In Figure 2b, the cluster assumption is violated and there are no density differences in the set of unsupervised samples. In this case, the consistency loss does more harm than good — even though it successfully flattens the neighborhood of the decision function, it does so also across the true class boundary. In order for the consistency regularization to be a net win, it would have to perturb the samples as much as possible, but at the same time avoid crossing the true class boundary.

In Figure 2c, we plot the contours of the distance to the true class boundary, suggesting a potentially better mechanism for perturbation. Indeed, when perturbations are done only along these contours, the probability of crossing the true class boundary is negligible compared to the regularization potential in the remaining dimension. Figure 2d shows that the resulting learned decision boundary aligns well with the true class boundary.

Low-density regions provide an effective signal that guides consistency regularization by providing areas into which a decision boundary can settle. This illustrative toy example demonstrates an alternative mechanism; the orientation of the decision boundary can be constrained to lie parallel to the directions of perturbation. We therefore argue that consistency regularization can be successful even when the cluster assumption is violated, if the following guidelines are observed: 1) the perturbations must be varied and high-dimensional in order to cover as much of the input space in the same class as possible, 2) the probability of a perturbation crossing the true class boundary must be very small compared to the amount of exploration in other dimensions, and 3) the perturbed inputs should be plausible, i.e., they should not be grossly outside the manifold of real inputs.

3.3 CUTOUT AND CUTMIX FOR SEMANTIC SEGMENTATION

If we consider the classical augmentation-like perturbations such as translation, rotation, scaling, and brightness/contrast changes, it is evident that these have a low chance of confusing the output class (Athiwaratkun et al., 2019) but they also provide very little variation. Note that in context of semantic segmentation, all geometric transformations need to be applied in reverse for the result image before computing the loss (Ji et al., 2018). As such, translation turns into a no-op, unlike in classification tasks where it remains a useful perturbation. Adding noise is another questionable
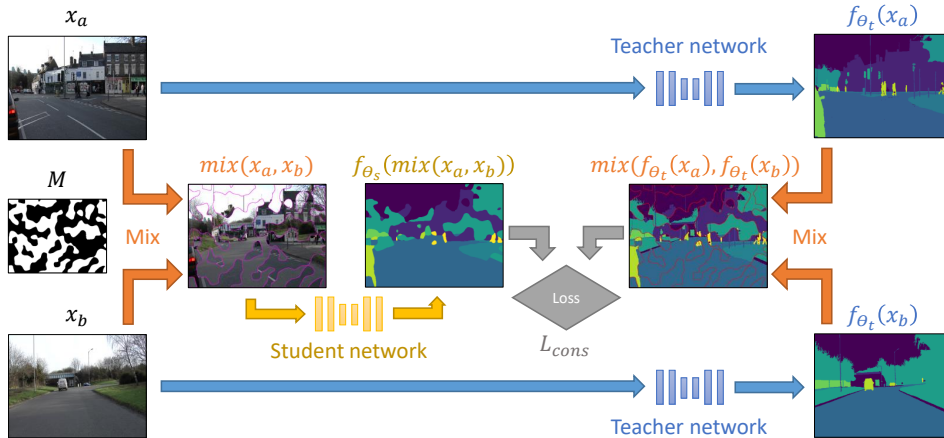
Figure 3: Illustration of mixing regularization for semi-supervised semantic segmentation with the mean teacher framework. θ_s and θ_t denote the weights of the student and teacher networks, respectively. The arbitrary mask M is omitted from the argument list of function mix for legibility.

perturbation strategy — although high-dimensional, such perturbations are very unlikely to lie on the manifold of natural images.

Out of previously proposed perturbation methods for consistency regularization, we identify CutOut and CutMix as promising candidates for semantic segmentation as they provide a large variety of possible outputs and are class preserving. Both approaches use a mask M with a randomly chosen rectangular region. Our masks have $M = 1$ inside the rectangle, and $M = 0$ otherwise.

CutOut.   To apply CutOut in a semantic segmentation task, we mask the input pixels with M and disregard the consistency loss for pixels masked to 0 by M. Using square distance as the metric, we have $L_{cons} = \|M \odot (f_\theta(M \odot x) - f_\theta(x))\|^2$, where $\odot$ denotes an elementwise product.

CutMix.   CutMix requires two input images that we shall denote x_a and x_b that we mix with the mask M. Following ICT (Verma et al. (2019)) we run both input images as well as the mixed variant through the network. The consistency loss is then taken between the segmentation of the mixed image and the mix between the segmented input images. To simplify the notation, let us define function $mix(a, b, M) = (1 - M) \odot a + M \odot b$ that selects the output pixel based on mask M. We can now write the consistency loss for segmentation CutMix as

$$L_{cons} = \big\|mix\big(f_\theta(x_a), f_\theta(x_b), M\big) - f_\theta\big(mix(x_a, x_b, M)\big)\big\|^2. \tag{2}$$

So far we have assumed that both original and perturbed images are segmented using the same network f_θ. In this sense, our approach is similar to the Π-network Laine & Aila (2017), although mean teacher (Tarvainen & Valpola, 2017) is known to outperform it in image classification tasks. Our preliminary tests indicated that the same is true for semantic segmentation, and therefore all the experiments in this paper use the mean teacher framework. Specifically, in CutOut, we segment the unperturbed image x using the teacher network and the perturbed image $M \odot x$ using the student network. In CutMix — following Verma et al. (2019) — we similarly segment the original images x_a and x_b using the teacher network, and the mixed image using the student network. The computation is illustrated in Figure 3.

To analyze how much variation these perturbations provide, we note that the original CutOut always masks out a fixed-size square at a random position, so the resulting mask has only two degrees of freedom. The original CutMix has three degrees of freedom in choosing the position and size of the rectangle (the aspect ratio is fixed), and in addition it replaces the contents of the rectangle from another training image, providing one further degree of freedom. Probably more importantly, the CutOut-perturbed images are rather implausible because real data rarely contains axis-aligned constant-color rectangles, whereas the content-filled rectangles of CutMix are not nearly as conspicuous. In semantic segmentation, we deviate from the original methods in that we choose all four parameters of the rectangle at random in order to obtain as much variation as possible.
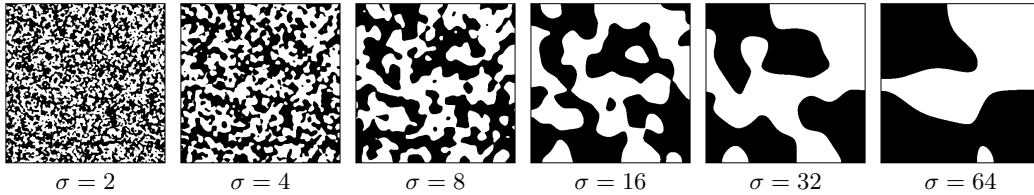
5

Figure 4: Example CowOut/CowMix masks with $p = 0.5$ and varying σ in a 384×384 pixel image.

3.4 CowOut and CowMix

The use of a rectangular mask restricts the dimensionality of the perturbations that CutOut and CutMix can produce. Intuitively, a more complex mask that has more degrees of freedom should provide better exploration of the plausible input space. We propose combining the semantic CutOut and CutMix regularizers introduced above with a novel mask generation method, giving rise to two regularization methods that we dub CowOut and CowMix due to the Friesian cow -like texture of the masks.

To generate a mask with a given proportion p of pixels having $M = 0$, we start by sampling a Gaussian noise image $\mathcal{N}(0, I)$, convolve it with a Gaussian smoothing kernel, and threshold the result at $\tau = \mathrm{erf}^{-1}(2p - 1)\sqrt{2}S_\sigma + S_\mu$, where S_μ and S_σ are the mean and standard deviation of the smoothed noise, respectively. The standard deviation σ of the Gaussian smoothing kernel determines the average size of features in the mask and is drawn from a log-uniform distribution: $\sigma \sim \log \mathcal{U}(\sigma_{min}, \sigma_{max})$. Figure 4 shows example masks with varying values of σ.

To estimate how much variation these masks contain, we first observe that if no smoothing were performed before thresholding, we would obtain a binary per-pixel Bernoulli mask. This has an exponential amount of variation with respect to the area of the receptive field: a receptive field with area A has 2^A possible masks. Applying the smoothing filter has a similar effect as zooming the mask — if the smoothing constant σ is doubled, we can expect to obtain roughly 4× fewer "bits" of variation (see, e.g., Figure 4, $\sigma = 8$ vs. $\sigma = 16$). The suitable value for σ is thus an empirical tradeoff between the amount of variation, i.e., the strength of the resulting perturbation, and plausibility of the masked/mixed image. If too little filtering is performed, we obtain a huge amount of variation but the perturbed images are unrealistic, and with too much filtering the images are very realistic but the amount of variation is small. As a geometric interpretation, we hypothesize that the more varied masks help the network to cope with occlusions better than the rectangular masks that can mimic occlusions only along horizontal and vertical edges.

Considering potential future work, we note that it should be possible to improve the results further with a more principled method for choosing σ so that its distribution is automatically adapted to the training data.

4 Experiments

We will now describe describe our experiments and main results. We will start by describing the training setup, followed by an investigation of various perturbation methods in the context of semi-supervised semantic segmentation, and conclude with a comparison against the state-of-the-art.

4.1 Training setup

We use two segmentation networks in our experiments: 1) U-Net (Ronneberger et al., 2015) with a ResNet-50 (He et al., 2016) based encoder that was pre-trained using ImageNet and a randomly initialized decoder (Appendix C.2), and 2) DeepLab v2 network (Chen et al., 2017) based on ResNet-101 and pre-trained for semantic segmentation using the COCO (Lin et al., 2014) dataset, as used by Hung et al. (2018).

Our implementation uses the PyTorch framework, Adam (Kingma & Ba, 2015) optimizer, and the mean teacher algorithm (Tarvainen & Valpola, 2017), as detailed in Appendix C.3. We replace the sigmoidal ramp-up of the consistency regularization weight (Laine & Aila, 2017; Tar-

Sup. baseline	Std. aug[a]	ICT	Cutout	CutMix[b]	CowOut	CowMix	Fully sup.
$48.66\% \pm 1.80$	$46.24\% \pm 2.21$	$48.29\% \pm 2.01$	$53.09\% \pm 2.56$	$50.95\% \pm 2.49$	$52.93\% \pm 1.35$	$\mathbf{55.06\%} \pm 1.74$	$64.19\% \pm 0.41$

Table 1: Measurements and ablation on CAMVID test set. Our results are mean intersection-over-union (mIoU) presented as $mean \pm std.dev$ computed from 10 runs. Training was run for 300 epochs, except in (a) standard augmentation and (b) CutMix experiments where convergence failures were observed. For those experiments, the results were taken after (a) 50 and (b) 100 epochs.

vainen & Valpola, 2017) using the average thresholded confidence of the teacher network (see Appendix C.3.4), which automatically increases as the training progresses (French et al., 2018). We will make our implementation available.

4.2 COMPARISON OF PERTURBATION METHODS

The CAMVID (Brostow et al., 2008) training set consists of 367 images. We chose 10 subsets of 30 labeled images that were used for the supervised loss, while all training images were used to compute the consistency loss. The U-net setup is used in this test.

The results for different perturbation methods are given in Table 1. Perturbations based on standard data augmentation (flips, rotations, brightness, etc., see Appendix C.1) and Interpolation Consistency Training (ICT) resulted in no measurable improvement in the mean IoU score compared to the baseline of supervised training using only the labeled samples. The Cutout and CutMix experiments used masks with a single random rectangle, and led to clear improvements over the baseline.

For CowOut and CowMix, we generated the masks using $\sigma \in [4, 16]$. For CowOut, we found that choosing the masked pixel proportion randomly with $p \sim \mathcal{U}(0, 1)$ produced the best results, whereas for CowMix it was optimal to always use $p = 0.5$. CowMix led to the best result in this experiment, bridging approximately half of the gap between the supervised baseline and the fully supervised reference result.

We tuned all hyper-parameters using the CAMVID dataset due to its small size and fast run-time. We found that these hyper-parameters also worked well for other, larger datasets.

4.3 RESULTS ON CITYSCAPES AND PASCAL VOC

We will now compare our results against the state-of-the-art in semi-supervised semantic segmentation, which is currently the adversarial training approach of Hung et al. (2018). We use two datasets in our experiments. CITYSCAPES consists of urban scenery captured from the perspective of a vehicle. Its training set consists of 2975 images. PASCAL VOC 2012 (Everingham et al., 2012) is more varied, but includes only 1464 training images, and thus we follow the lead of Hung et al. and augment it using SEMANTIC BOUNDARIES (Hariharan et al., 2011), resulting in 10582 training images. We note that we generated CowMix masks using $\sigma \in [8, 32]$ due to the larger visual features present in CITYSCAPES and PASCAL VOC.

Our results are given in Tables 2 and 3 as mean intersection-over-union (mIoU) percentages, where higher is better. The supervised baseline results between Hung et al. and our DeepLab implementation are based on the same setup, provided by the authors, but differ slightly in practice due to the different choice of optimizer, etc.

We can see that using the same DeepLab setup, CowMix outperforms the adversarial training approach in both datasets, with the exception of PASCAL when using a large number of labeled samples. The difference is particularly significant when only a small number of labeled samples is available, e.g., 52% vs 38% mIoU with 100 labeled samples in PASCAL.

When using our U-Net architecture — in which the decoder *has not been pre-trained* — we were unable to successfully apply the adversarial approach. U-Net improves the performance of CowMix on CITYSCAPES and continues to yield significant gains relative to the supervised baseline in the case of PASCAL. While the performance on the more varied PASCAL dataset significantly benefits the pre-training of DeepLab v2, it also provides a good test environment for semi-supervised learning algorithms when the decoder is randomly initialized.

Labeled samples	**100**	**372 (12.5%)**	**744 (25%)**	**1488 (50%)**	**2975 (All)**
	Hung et al. (2018): Adversarial training with DeepLab v2 network and COCO-pretrained decoder				
Baseline	—	55.5%	59.9%	64.1%	66.4%
Semi-supervised	—	58.8%	62.3%	65.7%	—
Delta	—	3.5	2.4	1.6	—
	Our results: Same DeepLab v2 network and COCO-pretrained decoder				
Baseline	$44.34\%_{\pm 1.61}$	$56.02\%_{\pm 0.80}$	$60.90\%_{\pm 0.70}$	$65.05\%_{\pm 0.71}$	$67.79\%_{\pm 0.32}$
CowMix	$49.01\%_{\pm 2.58}$	$60.53\%_{\pm 0.29}$	$64.10\%_{\pm 0.82}$	$66.51\%_{\pm 0.45}$	$69.03\%_{\pm 0.27}$
Delta	4.67	4.51	3.20	1.46	1.24
	Our results: U-Net and randomly initialized decoder				
Baseline	$43.83\%_{\pm 0.99}$	$54.76\%_{\pm 0.50}$	$60.35\%_{\pm 0.93}$	$64.93\%_{\pm 0.32}$	$68.34\%_{\pm 0.76}$
CowMix	$\mathbf{51.98\%}_{\pm 2.76}$	$\mathbf{61.48\%}_{\pm 1.84}$	$\mathbf{64.85\%}_{\pm 0.26}$	$\mathbf{66.90\%}_{\pm 0.22}$	$\mathbf{69.57\%}_{\pm 0.43}$
Delta	8.15	6.72	4.50	1.97	1.23

Table 2: Performance (mIoU) on CITYSCAPES validation set, each computed from 5 runs. The results for Hung et al. (2018) are from their paper.

# Labels	**100**	**200**	**400**	**800**	**2646 (25%)**	**10582 (All)**
	Hung et al. (2018): Adversarial training with DeepLab v2 network and COCO-pretrained decoder					
Baseline	$39.22\%_{\pm 2.08}$	$46.57\%_{\pm 1.34}$	$55.65\%_{\pm 0.88}$	$62.54\%_{\pm 0.45}$	$68.41\%_{\pm 0.29}$	$72.50\%_{\pm 0.27}$
Semi-sup.	$38.82\%_{\pm 3.91}$	$49.40\%_{\pm 1.00}$	$60.29\%_{\pm 2.25}$	$66.45\%_{\pm 0.69}$	$\mathbf{71.27\%}_{\pm \mathbf{0.26}}$	—
Delta	0.40	2.83	4.64	3.91	2.86	—
	Our results: Same DeepLab v2 network and COCO-pretrained decoder					
Baseline	$41.17\%_{\pm 1.96}$	$48.96\%_{\pm 1.70}$	$58.18\%_{\pm 1.16}$	$64.51\%_{\pm 0.85}$	$70.16\%_{\pm 0.35}$	$73.32\%_{\pm 0.19}$
CowMix	$\mathbf{52.10\%}_{\pm 1.35}$	$\mathbf{57.84\%}_{\pm 1.55}$	$\mathbf{64.18\%}_{\pm 1.79}$	$\mathbf{67.84\%}_{\pm 0.88}$	$70.99\%_{\pm 0.41}$	$\mathbf{73.43\%}_{\pm 0.06}$
Delta	10.93	8.88	6.00	3.33	0.83	0.11
	Our results: U-Net and randomly initialized decoder					
Baseline	$24.91\%_{\pm 2.13}$	$33.66\%_{\pm 1.64}$	$41.80\%_{\pm 1.15}$	$49.18\%_{\pm 1.61}$	$60.58\%_{\pm 0.77}$	$65.97\%_{\pm 1.11}$
CowMix	$41.00\%_{\pm 2.70}$	$49.42\%_{\pm 1.74}$	$54.20\%_{\pm 1.12}$	$54.67\%_{\pm 5.66}$	$63.48\%_{\pm 0.26}$	$65.54\%_{\pm 4.99}$
Delta	16.09	15.76	12.4	5.49	2.90	-0.43

Table 3: Performance (mIoU) on augmented PASCAL VOC validation set, each computed from 5 runs.

4.4 DISCUSSION

We attribute the fact that the adversarial approach (Hung et al. (2018)) is ineffective with small numbers of labeled samples to the requirements imposed by its discriminator network. A small set of ground truth labels lacks the variation necessary to effectively train the discriminator to distinguish ground truth from predicted segmentation maps, preventing it from effectively guiding the segmentation network. In contrast, consistency regularization minimizes variation in prediction over class preserving perturbation, effectively propagating labels between unlabelled samples. It therefore does not impose similar requirements on the size of the labeled data set.

5 CONCLUSIONS

We have shown that consistency regularization is a viable solution for semi-supervised semantic segmentation, despite the lack of low-density regions between classes. The proposed CowMix regularization leads to very high-dimensional perturbations that enable state-of-the-art results, while being considerably easier to implement and use than the previous methods based on adversarial training. Even better and more varied perturbation strategies are an obvious avenue for future work. Additionally, it could be fruitful to investigate when the CowMix approach could also be beneficial in the context of classification.

REFERENCES

Ben Athiwaratkun, Marc Finzi, Pavel Izmailov, and Andrew Gordon Wilson. There are many consistent explanations of unlabeled data: Why you should average. In *International Conference on Learning Representations*, 2019.

Vijay Badrinarayanan, Alex Kendall, and Roberto Cipolla. Segnet: A deep convolutional encoder-decoder architecture for image segmentation. *CoRR*, abs/1511.00561, 2015.

David Berthelot, Nicholas Carlini, Ian Goodfellow, Nicolas Papernot, Avital Oliver, and Colin Raffel. Mixmatch: A holistic approach to semi-supervised learning. *CoRR*, abs/1905.02249, 2019.

Gabriel J. Brostow, Julien Fauqueur, and Roberto Cipolla. Semantic object classes in video: A high-definition ground truth database. *Pattern Recognition Letters*, 30(2):88–97, 2008.

Olivier Chapelle and Alexander Zien. Semi-supervised classification by low density separation. In *AISTATS*, volume 2005, pp. 57–64, 2005.

Liang-Chieh Chen, George Papandreou, Iasonas Kokkinos, Kevin Murphy, and Alan L Yuille. Semantic image segmentation with deep convolutional nets and fully connected crfs. *CoRR*, abs/1412.7062, 2014.

Liang-Chieh Chen, George Papandreou, Iasonas Kokkinos, Kevin Murphy, and Alan L Yuille. Deeplab: Semantic image segmentation with deep convolutional nets, atrous convolution, and fully connected CRFs. *IEEE transactions on pattern analysis and machine intelligence*, 40(4): 834–848, 2017.

Terrance DeVries and Graham W Taylor. Improved regularization of convolutional neural networks with cutout. *CoRR*, abs/1708.04552, 2017.

M. Everingham, L. Van Gool, C. K. I. Williams, J. Winn, and A. Zisserman. The PASCAL Visual Object Classes Challenge 2012 (VOC2012) Results, 2012.

Geoff French, Michal Mackiewicz, and Mark Fisher. Self-ensembling for visual domain adaptation. In *International Conference on Learning Representations*, 2018.

Bharath Hariharan, Pablo Arbeláez, Lubomir Bourdev, Subhransu Maji, and Jitendra Malik. Semantic contours from inverse detectors. In *International Conference on Computer Vision*, pp. 991–998, 2011.

Kaiming He, Xiangyu Zhang, Shaoqing Ren, and Jian Sun. Deep residual learning for image recognition. In *IEEE Conference on Computer Vision and Pattern Recognition*, pp. 770–778, 2016.

Wei-Chih Hung, Yi-Hsuan Tsai, Yan-Ting Liou, Yen-Yu Lin, and Ming-Hsuan Yang. Adversarial learning for semi-supervised semantic segmentation. *CoRR*, abs/1802.07934, 2018.

Xu Ji, João F. Henriques, and Andrea Vedaldi. Invariant information distillation for unsupervised image segmentation and clustering. *CoRR*, abs/1807.06653, 2018.

Tarun Kalluri, Girish Varma, Manmohan Chandraker, and CV Jawahar. Universal semi-supervised semantic segmentation. *CoRR*, abs/1811.10323, 2018.

Diederik Kingma and Jimmy Ba. Adam: A method for stochastic optimization. In *International Conference on Learning Representations*, 2015.

Samuli Laine and Timo Aila. Temporal ensembling for semi-supervised learning. In *International Conference on Learning Representations*, 2017.

Tsung-Yi Lin, Michael Maire, Serge Belongie, James Hays, Pietro Perona, Deva Ramanan, Piotr Dollár, and C Lawrence Zitnick. Microsoft coco: Common objects in context. In *European conference on computer vision*, pp. 740–755, 2014.

Jonathan Long, Evan Shelhamer, and Trevor Darrell. Fully convolutional networks for semantic segmentation. In *IEEE Conference on Computer Vision and Pattern Recognition*, pp. 3431–3440, 2015.

Yucen Luo, Jun Zhu, Mengxi Li, Yong Ren, and Bo Zhang. Smooth neighbors on teacher graphs for semi-supervised learning. In *IEEE Conference on Computer Vision and Pattern Recognition*, pp. 8896–8905, 2018.

Takeru Miyato, Schi-ichi Maeda, Masanori Koyama, and Shin Ishii. Virtual adversarial training: a regularization method for supervised and semi-supervised learning. *arXiv preprint arXiv:1704.03976*, 2017.

Mohammadreza Mostajabi, Payman Yadollahpour, and Gregory Shakhnarovich. Feedforward semantic segmentation with zoom-out features. *CoRR*, abs/1412.0774, 2014.

Avital Oliver, Augustus Odena, Colin Raffel, Ekin D. Cubuk, and Ian J. Goodfellow. Realistic evaluation of semi-supervised learning algorithms. In *International Conference on Learning Representations*, 2018.

Christian S Perone and Julien Cohen-Adad. Deep semi-supervised segmentation with weight-averaged consistency targets. In *Deep Learning in Medical Image Analysis and Multimodal Learning for Clinical Decision Support*, pp. 12–19. Springer, 2018.

Boris T Polyak and Anatoli B Juditsky. Acceleration of stochastic approximation by averaging. *SIAM Journal on Control and Optimization*, 30(4):838–855, 1992.

Olaf Ronneberger, Philipp Fischer, and Thomas Brox. U-net: Convolutional networks for biomedical image segmentation. In *International Conference on Medical Image Computing and Computer-Assisted Intervention*, pp. 234–241, 2015.

Mehdi Sajjadi, Mehran Javanmardi, and Tolga Tasdizen. Mutual exclusivity loss for semi-supervised deep learning. In *23rd IEEE International Conference on Image Processing, ICIP 2016*, 2016a.

Mehdi Sajjadi, Mehran Javanmardi, and Tolga Tasdizen. Regularization with stochastic transformations and perturbations for deep semi-supervised learning. In *Advances in Neural Information Processing Systems*, pp. 1163–1171, 2016b.

Rui Shu, Hung Bui, Hirokazu Narui, and Stefano Ermon. A DIRT-t approach to unsupervised domain adaptation. In *International Conference on Learning Representations*, 2018.

K. Simonyan and A. Zisserman. Very deep convolutional networks for large-scale image recognition. *CoRR*, abs/1409.1556, 2014.

Sinisa Stekovic, Friedrich Fraundorfer, and Vincent Lepetit. S4-net: Geometry-consistent semi-supervised semantic segmentation. *CoRR*, abs/1812.10717, 2018.

Antti Tarvainen and Harri Valpola. Mean teachers are better role models: Weight-averaged consistency targets improve semi-supervised deep learning results. In *Advances in Neural Information Processing Systems*, pp. 1195–1204, 2017.

Vikas Verma, Alex Lamb, Juho Kannala, Yoshua Bengio, and David Lopez-Paz. Interpolation consistency training for semi-supervised learning. *CoRR*, abs/1903.03825, 2019.

Sangdoo Yun, Dongyoon Han, Seong Joon Oh, Sanghyuk Chun, Junsuk Choe, and Youngjoon Yoo. Cutmix: Regularization strategy to train strong classifiers with localizable features. *CoRR*, abs/1905.04899, 2019.

Hongyi Zhang, Moustapha Cisse, Yann N. Dauphin, and David Lopez-Paz. mixup: Beyond empirical risk minimization. In *International Conference on Learning Representations*, 2018.

A   2D TOY EXPERIMENTS

The neural networks used in our 2D toy experiments are simple classifiers in which samples are 2D x, y points ranging from -1 to 1. Our networks are multi-layer perceptrons consisting of 3 hidden layers of 512 units, each followed by a ReLU non-linearity. The final layer is a 2-unit classification layer. We use the mean teacher (Tarvainen & Valpola, 2017) semi-supervised learning algorithm with binary cross-entropy as the consistency loss function, a consistency loss weight of 10 and confidence thresholding (French et al., 2018) with a threshold of 0.97. The ground truth decision boundary was derived from a hand-drawn 512×512 pixel image.

The constrained consistency regularization experiment described in Section 3.2 required that a sample x should be perturbed to $\hat{x}$ such that they are at the same — or similar — distance to the ground truth decision boundary. This was achieved by drawing isotropic perturbations from a normal distrubtion $\hat{x} = x + h$ where $h \sim \mathcal{N}(0, 0.117)$ (0.117 $\approx$ 30 pixels in the source image), determining the distances $m(x)$ and $m(\hat{x})$ from x and $\hat{x}$ to the ground truth boundary (using a pre-computed distance map) and discarding the perturbation – by masking consistency loss for x to 0 – if $|m(\hat{x}) - m(x)| > 0.016$ (0.016 $\approx$ 4 pixels in the source image).

B   PSEUDOCODE

The mask generation function is given in the form of Python/PyTorch code in Listing 1, and the training functions for semi-supervised CutOut and CutMix are given in Listings 2 and 3, respectively. The latter incorporate the mean teacher framework (Tarvainen & Valpola, 2017) and confidence thresholding (French et al., 2018) as used in our experiments. In keeping with Yun et al. (2019); DeVries & Taylor (2017); Verma et al. (2019), our mask generator allows the proportion of pixels that come from each source image to vary. Although we found via experimentation that for CowMix the best proportion was always $p = 0.5$, varying the proportion is beneficial for CowOut as detailed in Section 4.2.

```python
import numpy as np
from scipy.ndimage.filter import gaussian_filter
from scipy.special import erfinv

def generate_mixing_mask(img_size, sigma_min, sigma_max, p_min, p_max):
  # Randomly draw sigma from log-uniform distribution
  sigma = np.exp(np.random.uniform(np.log(sigma_min), np.log(sigma_max)))
  p = np.random.uniform(p_min, p_max)        # Randomly draw proportion p
  N = np.random.normal(size=img_size)        # Generate noise image
  Ns = gaussian_filter(N, sigma)             # Smooth with a Gaussian
  # Compute threshold
  t = erfinv(p*2 - 1) * (2**0.5) * Ns.std() + Ns.mean()
  return (noise_smooth > t).astype(float)  # Apply threshold and return
```
Listing 1: Python/NumPy code for cow mask generation

```python
def cutout_loss(x, mask, teacher_model, student_model):
  """x is input image of shape (batch, chan, H, W), mask is mixing mask
     of shape (batch, 1, H, W)"""
  # Apply teacher model and softmax to get per-pixel class probability
  y_t = softmax(teacher_model(x), dim=1)
  # Apply student model to masked image
  y_s = softmax(student_model(x * mask), dim=1)
  # Confidence thresholding factor
  confidence = y_t.max(dim=1) # Dimension 1 is class prob.
  conf_fac = (confidence > 0.97).mean()
  # Consistency is squared error between student and teacher preds for
    masked pixels only, modulated with confidence factor
  return (squared_diff(ym_t, ym_s) * m).mean() * conf_fac
```
Listing 2: PyTorch code for CutOut / CowOut for segmentation

```python
def cutmix_loss(xa, xb, mask, teacher_model, student_model):
```
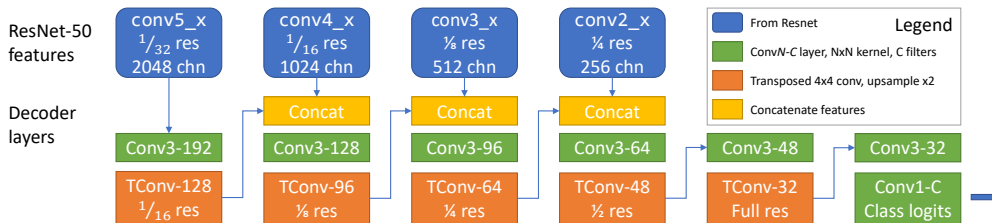
Figure 5: ResNet-50 based U-Net decoder architecture.

```python
"""xa, xb are input image pair each of shape (batch, chan, H, W), mask
    is mixing mask of shape (batch, 1, H, W)"""
# Apply teacher model and softmax to get per-pixel class probability
ya_t = softmax(teacher_model(xa), dim=1)
yb_t = softmax(teacher_model(yb), dim=1)
# Mix images and teacher predictions
xm = xa * (1 - mask) + xb * mask
ym_t = ya_t * (1 - mask) + yb_t * mask
# Apply student model to mixed image
ym_s = softmax(student_model(xm), dim=1)
# Confidence thresholding factor
confidence = ym_t.max(dim=1) # Dimension 1 is class prob.
conf_fac = (confidence > 0.97).mean()
# Consistency is squared error between student and teacher preds,
    modulated with confidence factor
return squared_diff(ym_t, ym_s).mean() * conf_fac
```

Listing 3: PyTorch code for CutMix / CowMix for segmentation

C   SEMANTIC SEGMENTATION EXPERIMENTS

C.1   DATA AUGMENTATION

Our data augmentation scheme that we used for standard augmentation based perturbation consists of an affine transformation composed of horizontal flips, translation in the range $[-4, 4]$ pixels, uniform scaling in the range $[0.8, 1.25]$ and rotation in the range $[-15°, 15°]$. We also modify the brightness and contrast by adding a value $b \sim \mathcal{N}(0, 0.1)$ and scaling by a factor $c \sim e^{\mathcal{N}(0, ln(1.1))}$.

C.2   U-NET NETWORK ARCHITECTURE

Our U-Net network is shown in Figure 5 and Table 4.

C.3   TRAINING DETAILS

C.3.1   EXPERIMENTS USING U-NET ARCHITECTURE

In keeping with Long et al. (2015) we use a batch size of 1. We freeze the batch normalization layers within the ResNet encoder, using the pre-trained running mean and variance rather than computing per-batch mean and variance during training. We use the Adam Kingma & Ba (2015) optimization algorithm with a learning rate of 1×10^{-4}. As per the mean teacher algorithm Tarvainen & Valpola (2017), after each iteration the weights w_t of the teacher network are updated to be the exponential moving average of the weights w_s of the student: $w_t = \alpha_t w_t + (1 - \alpha_t) w_s$, where $\alpha_t = 0.99$.

The Cityscapes images were downsampled to half resolution (1024×512) prior to use, as in Hung et al. (2018). When using Cityscapes we trained for 100,000 iterations using a batch size of 1.

Description	Resolution $\times$ channels
ResNet-50 layer `conv5_x` $\frac{1}{32}$ res, 2048 chn	$\frac{1}{32} \times 2048$
Conv $3 \times 3 \times 192$	$\frac{1}{32} \times 192$
TransposeConv $4 \times 4 \times 128$	$\frac{1}{16} \times 128$
Concat with ResNet-50 layer `conv4_x` $\frac{1}{16}$ res, 1024 chn	$\frac{1}{16} \times 1152$
Conv $3 \times 3 \times 128$	$\frac{1}{16} \times 128$
TransposeConv $4 \times 4 \times 96$	$\frac{1}{8} \times 96$
Concat with ResNet-50 layer `conv3_x` $\frac{1}{8}$ res, 512 chn	$\frac{1}{8} \times 608$
Conv $3 \times 3 \times 96$	$\frac{1}{8} \times 96$
TransposeConv $4 \times 4 \times 64$	$\frac{1}{4} \times 64$
Concat with ResNet-50 layer `conv2_x` $\frac{1}{4}$ res, 256 chn	$\frac{1}{4} \times 320$
Conv $3 \times 3 \times 64$	$\frac{1}{4} \times 64$
TransposeConv $4 \times 4 \times 48$	$\frac{1}{2} \times 48$
Conv $3 \times 3 \times 48$	$\frac{1}{2} \times 48$
TransposeConv $4 \times 4 \times 32$	1×32
Conv $3 \times 3 \times 32$	1×32
Conv $1 \times 1 \times C$	$1 \times C$

Table 4: ResNet-50 based U-Net decoder. C is the number of target classes.

We tuned our approach and selected hyper-parameters using the CAMVID dataset due to its small size and fast run-time, after which we applied the same hyper-parameters to Cityscapes. We did not run the augmentation based perturbation experiments on the Cityscapes dataset due to the long run-time involved.

C.3.2 EXPERIMENTS USING DEEPLAB V2 ARCHITECTURE

We found that we had to decrease the learning rate to 1×10^{-5} to get good performance with DeepLab v2. We note that the PyTorch implementation of DeepLab v3 worked best with 1×10^{-4}. We believe that this is because the U-Net and DeepLab v3 networks accept input images with zero-mean unit-variance, where DeepLab v2 accepts images whose values are in the range 0 to 255 with only mean subtraction.

For the PASCAL VOC experiments, we extracted 321×321 random crops and used a batch size of 10, in keeping with Hung et al. (2018). For the CITYSCAPES experiments we used full image crops and a batch size of 2.

C.3.3 ABLATION

The augmentation based perturbation experiments performed on the CAMVID dataset were trained for 50 epochs. The CutMix and CowOut experiments were trained for 100.

C.3.4 CONFIDENCE THRESHOLDING

French et al. (2018) apply confidence thresholding, in which they mask consistency loss to 0 for samples whose confidence as predicted by the teacher network is below a threshold of 0.968. In the context of segmentation, we found that this masks pixels close to class boundaries as they usually have a low confidence. These regions are often large enough to encompass small objects, preventing learning and degrading performance. Instead we modulate the consistency loss with the proportion of pixels whose confidence is above the threshold. This values grows throughout training, taking the place of the sigmoidal ramp-up used in Laine & Aila (2017); Tarvainen & Valpola (2017).

C.4 DETAILED PERFORMANCE TABLES

The detailed per-class performance on the CITYSCAPES dataset are presented in Table 5 and visualized in Figure 6, ad on the augmented PASCAL VOC dataset are presented in Table 6 and visualized in Figure 7.
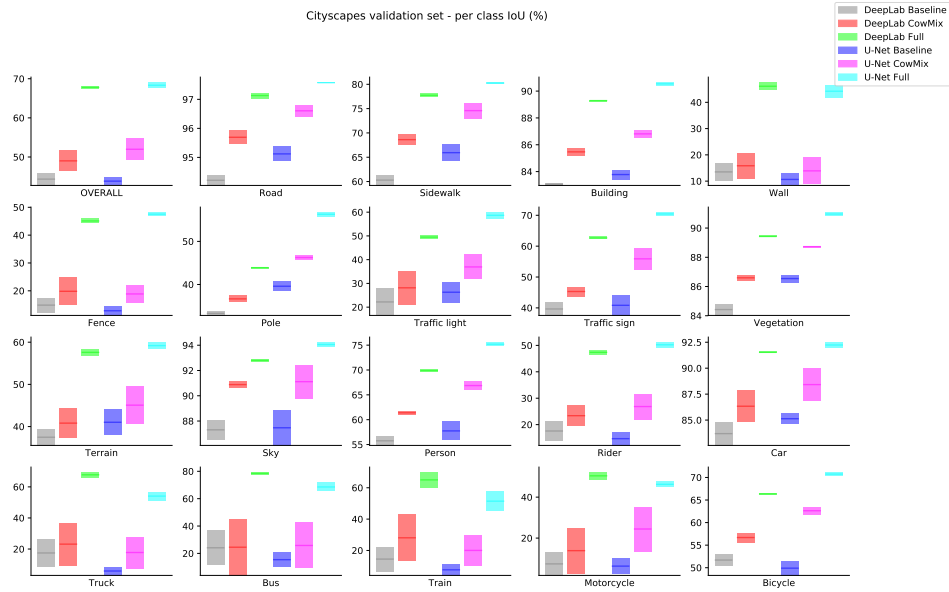
Figure 6: Visualization of semi-supervised segmentation on CITYSCAPES, 100 supervised samples
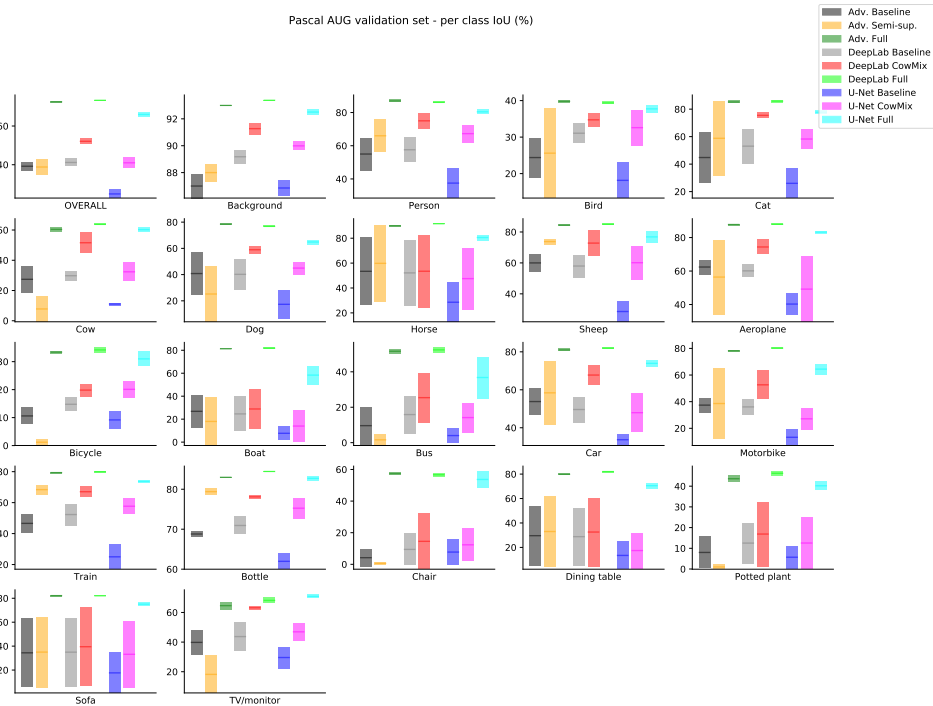

Figure 7: Visualization of semi-supervised segmentation on augmented PASCAL VOC dataset, 100 supervised samples

	OVERALL	Road	Sidewalk	Building
DeepLab Baseline	$44.34\% \pm 1.61$	$94.21\% \pm 0.18$	$60.29\% \pm 1.09$	$83.06\% \pm 0.09$
DeepLab CowMix	$49.01\% \pm 2.58$	$95.69\% \pm 0.24$	$68.62\% \pm 1.11$	$85.47\% \pm 0.30$
DeepLab Full	$67.79\% \pm 0.32$	$97.13\% \pm 0.09$	$77.74\% \pm 0.36$	$89.29\% \pm 0.07$
U-net Baseline	$43.83\% \pm 0.99$	$95.12\% \pm 0.25$	$65.94\% \pm 1.74$	$83.78\% \pm 0.34$
U-net CowMix	$51.98\% \pm 2.76$	$96.61\% \pm 0.20$	$74.59\% \pm 1.57$	$86.81\% \pm 0.27$
U-net Full	$68.34\% \pm 0.76$	$97.57\% \pm 0.02$	$80.26\% \pm 0.16$	$90.54\% \pm 0.12$
	Wall	Fence	Pole	Traffic light
DeepLab Baseline	$13.51\% \pm 3.39$	$14.86\% \pm 2.63$	$33.31\% \pm 0.49$	$22.20\% \pm 5.68$
DeepLab CowMix	$15.85\% \pm 4.84$	$19.82\% \pm 4.89$	$36.66\% \pm 0.79$	$28.14\% \pm 7.10$
DeepLab Full	$46.12\% \pm 1.51$	$45.09\% \pm 0.88$	$43.91\% \pm 0.14$	$49.49\% \pm 0.73$
U-net Baseline	$10.65\% \pm 2.28$	$12.84\% \pm 1.67$	$39.59\% \pm 1.09$	$26.29\% \pm 4.40$
U-net CowMix	$13.91\% \pm 5.01$	$18.87\% \pm 3.07$	$46.25\% \pm 0.50$	$36.94\% \pm 5.18$
U-net Full	$44.22\% \pm 2.36$	$47.52\% \pm 0.69$	$56.29\% \pm 0.47$	$58.68\% \pm 1.28$
	Traffic sign	Vegetation	Terrain	Sky
DeepLab Baseline	$39.65\% \pm 2.08$	$84.42\% \pm 0.40$	$37.48\% \pm 1.94$	$87.30\% \pm 0.75$
DeepLab CowMix	$45.30\% \pm 1.48$	$86.60\% \pm 0.20$	$40.82\% \pm 3.46$	$90.88\% \pm 0.24$
DeepLab Full	$62.67\% \pm 0.39$	$89.42\% \pm 0.04$	$57.59\% \pm 0.79$	$92.80\% \pm 0.08$
U-net Baseline	$40.83\% \pm 3.27$	$86.54\% \pm 0.27$	$41.02\% \pm 3.02$	$87.47\% \pm 1.40$
U-net CowMix	$55.89\% \pm 3.44$	$88.73\% \pm 0.05$	$45.08\% \pm 4.41$	$91.12\% \pm 1.31$
U-net Full	$70.43\% \pm 0.55$	$90.96\% \pm 0.12$	$59.19\% \pm 0.80$	$94.05\% \pm 0.18$
	Person	Rider	Car	Truck
DeepLab Baseline	$55.76\% \pm 0.93$	$17.59\% \pm 3.70$	$83.70\% \pm 1.14$	$17.46\% \pm 8.96$
DeepLab CowMix	$61.39\% \pm 0.39$	$23.38\% \pm 3.80$	$86.33\% \pm 1.50$	$23.15\% \pm 13.60$
DeepLab Full	$69.89\% \pm 0.24$	$47.37\% \pm 0.76$	$91.52\% \pm 0.08$	$67.77\% \pm 1.65$
U-net Baseline	$57.75\% \pm 1.81$	$14.69\% \pm 2.56$	$85.13\% \pm 0.49$	$5.86\% \pm 2.83$
U-net CowMix	$66.86\% \pm 0.90$	$26.85\% \pm 4.78$	$88.42\% \pm 1.57$	$17.77\% \pm 10.13$
U-net Full	$75.18\% \pm 0.40$	$50.23\% \pm 0.96$	$92.23\% \pm 0.27$	$54.06\% \pm 2.89$
	Bus	Train	Motorcycle	Bicycle
DeepLab Baseline	$24.11\% \pm 12.62$	$14.49\% \pm 7.71$	$7.40\% \pm 5.63$	$51.69\% \pm 1.24$
DeepLab CowMix	$24.52\% \pm 20.60$	$28.07\% \pm 14.68$	$13.86\% \pm 11.17$	$56.69\% \pm 1.10$
DeepLab Full	$78.46\% \pm 0.86$	$65.02\% \pm 4.88$	$50.41\% \pm 1.75$	$66.36\% \pm 0.13$
U-net Baseline	$15.42\% \pm 5.23$	$7.65\% \pm 3.57$	$6.31\% \pm 3.76$	$49.90\% \pm 1.60$
U-net CowMix	$25.80\% \pm 16.62$	$20.02\% \pm 9.65$	$24.43\% \pm 10.97$	$62.63\% \pm 0.88$
U-net Full	$68.56\% \pm 3.08$	$51.44\% \pm 6.32$	$46.26\% \pm 1.31$	$70.74\% \pm 0.41$

Table 5: Per-class performance on CITYSCAPES dataset, 100 supervised samples

C.5 HYPER-PARAMETER CHOICE

We explored the hyper-parameters for CowMix using the CAMVID dataset. We present our results in the form of bar plots. Black and green bars at left and right end are the performance of the baseline and fully supervised setups respectively while blue bars show response to hyper-parameter values. The performance is strong when consistency weight has a value in the range of 3 to 30, with 10 being the optimum choice, as seen in Figure 8.

The EMA α value used to update the teacher network had little effect, as seen in Figure 9.

The σ used for Gaussian smoothing yielded good results when between 4 and 8, but was best when drawn from $\sigma \sim \log \mathcal{U}(4, 16)$, as seen in Figure 10.
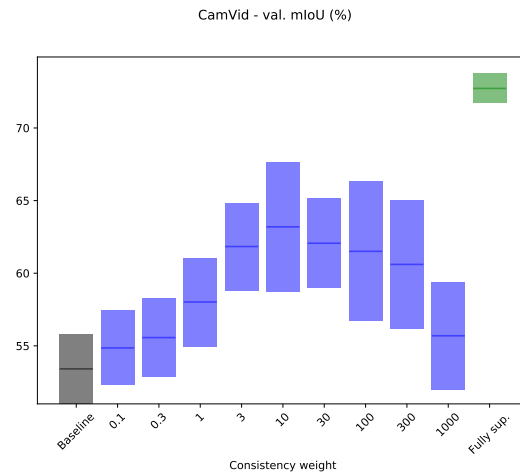
Figure 8: Effect of consistency weight hyper-parameter. In each bar, the central line is the mean, with the extents of the bar placed 1 standard deviation each side.
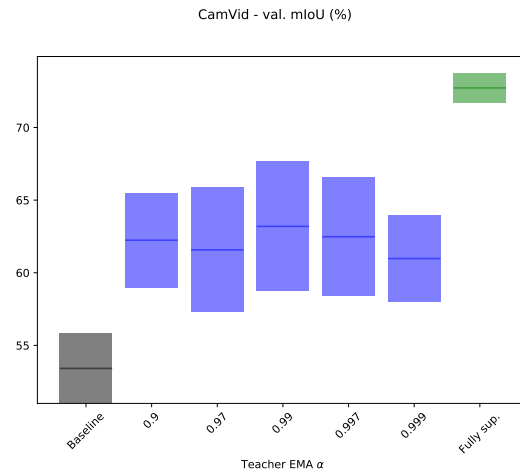

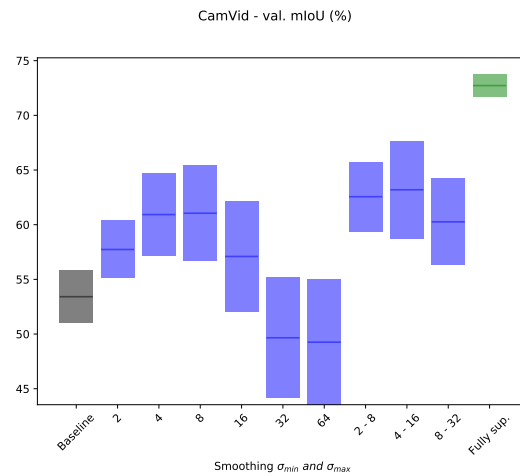Figure 9: Effect of mean teacher EMA hyper-parameter.

Figure 10: Effect of CowMix σ_{min} and σ_{max} hyper-parameters. A single value indicates that σ was fixed, while a range (e..g 4-16) indicates $\sigma \sim \log \mathcal{U}(4, 16)$.

	OVERALL	Background	Person	Bird
Adv. Baseline	39.22% ± 2.08	87.00% ± 0.89	55.00% ± 9.88	24.40% ± 5.46
Adv. Semi-sup.	38.82% ± 3.91	88.00% ± 0.63	66.00% ± 9.70	25.60% ± 12.22
Adv. Full	72.50% ± 0.27	93.00% ± 0.00	87.00% ± 0.63	39.80% ± 0.40
DeepLab Baseline	41.17% ± 1.96	89.18% ± 0.51	57.57% ± 7.40	31.07% ± 2.66
DeepLab CowMix	52.10% ± 1.35	91.27% ± 0.43	75.01% ± 4.77	34.73% ± 1.90
DeepLab Full	73.32% ± 0.19	93.39% ± 0.03	86.13% ± 0.39	39.36% ± 0.39
U-net Baseline	24.91% ± 2.13	86.85% ± 0.57	37.48% ± 9.01	18.15% ± 4.85
U-net CowMix	41.00% ± 2.70	89.99% ± 0.32	67.28% ± 5.26	32.59% ± 4.92
U-net Full	65.97% ± 1.11	92.50% ± 0.19	80.44% ± 1.45	37.74% ± 1.01
	Cat	Cow	Dog	Horse
Adv. Baseline	44.80% ± 18.54	27.40% ± 8.64	40.80% ± 16.27	53.40% ± 27.22
Adv. Semi-sup.	58.80% ± 26.95	7.80% ± 8.47	25.20% ± 21.17	59.80% ± 30.72
Adv. Full	85.20% ± 0.98	60.40% ± 1.62	78.40% ± 0.49	90.00% ± 0.63
DeepLab Baseline	53.06% ± 12.50	29.79% ± 3.06	40.19% ± 11.65	52.14% ± 26.38
DeepLab CowMix	75.49% ± 2.11	51.59% ± 6.62	58.94% ± 2.76	53.47% ± 29.03
DeepLab Full	85.84% ± 0.91	63.73% ± 0.52	76.76% ± 0.44	91.58% ± 0.17
U-net Baseline	26.02% ± 10.70	11.06% ± 0.69	17.34% ± 10.69	28.56% ± 15.70
U-net CowMix	58.26% ± 7.16	32.37% ± 6.23	44.96% ± 4.58	47.54% ± 24.69
U-net Full	77.76% ± 1.16	60.25% ± 1.48	64.85% ± 1.60	80.54% ± 2.36
	Sheep	Aeroplane	Bicycle	Boat
Adv. Baseline	60.00% ± 5.76	62.40% ± 4.45	10.60% ± 3.01	26.80% ± 14.23
Adv. Semi-sup.	73.80% ± 1.72	56.40% ± 22.29	1.20% ± 1.17	18.00% ± 20.94
Adv. Full	84.40% ± 0.49	87.80% ± 0.40	33.40% ± 0.49	81.20% ± 0.40
DeepLab Baseline	57.98% ± 7.31	60.11% ± 3.79	14.76% ± 2.50	24.58% ± 15.00
DeepLab CowMix	72.81% ± 8.10	74.37% ± 4.38	19.83% ± 2.28	28.86% ± 17.15
DeepLab Full	84.97% ± 0.46	87.92% ± 0.42	34.19% ± 0.94	81.80% ± 0.78
U-net Baseline	28.57% ± 6.63	40.27% ± 6.37	9.18% ± 3.09	7.68% ± 5.95
U-net CowMix	60.13% ± 10.67	49.20% ± 19.50	20.10% ± 2.95	13.99% ± 13.67
U-net Full	76.83% ± 3.57	83.25% ± 0.81	30.99% ± 2.60	58.35% ± 8.13
	Bus	Car	Motorbike	Train
Adv. Baseline	9.60% ± 10.59	53.80% ± 6.91	37.40% ± 5.57	46.60% ± 5.99
Adv. Semi-sup.	1.60% ± 3.20	58.40% ± 16.80	38.60% ± 26.44	68.40% ± 2.94
Adv. Full	51.60% ± 1.20	81.00% ± 0.63	78.20% ± 0.75	79.40% ± 0.49
DeepLab Baseline	15.86% ± 10.62	49.61% ± 6.59	36.08% ± 5.83	52.30% ± 6.91
DeepLab CowMix	25.41% ± 14.08	67.77% ± 5.12	52.66% ± 10.88	67.04% ± 3.32
DeepLab Full	52.38% ± 1.46	81.93% ± 0.46	80.22% ± 0.61	79.96% ± 0.46
U-net Baseline	4.00% ± 4.00	33.70% ± 3.04	13.26% ± 6.16	24.99% ± 8.00
U-net CowMix	14.15% ± 8.28	47.94% ± 10.07	27.13% ± 8.12	57.67% ± 4.95
U-net Full	36.78% ± 11.81	73.91% ± 1.66	64.44% ± 3.96	73.71% ± 0.78
	Bottle	Chair	Dining table	Potted plant
Adv. Baseline	68.80% ± 0.75	4.20% ± 5.38	29.60% ± 24.42	8.00% ± 7.67
Adv. Semi-sup.	79.40% ± 0.80	0.60% ± 0.80	33.00% ± 28.93	1.00% ± 1.10
Adv. Full	83.00% ± 0.00	57.40% ± 0.80	79.80% ± 0.75	43.60% ± 1.62
DeepLab Baseline	70.93% ± 2.15	9.44% ± 9.85	28.80% ± 23.68	12.51% ± 9.71
DeepLab CowMix	78.10% ± 0.39	14.53% ± 17.63	32.57% ± 28.15	16.88% ± 15.62
DeepLab Full	84.45% ± 0.11	56.66% ± 1.03	82.06% ± 0.46	46.21% ± 1.11
U-net Baseline	61.96% ± 1.97	7.75% ± 8.12	13.44% ± 11.28	5.69% ± 5.38
U-net CowMix	75.26% ± 2.51	12.34% ± 10.32	17.43% ± 14.52	12.55% ± 12.38
U-net Full	82.71% ± 0.54	53.68% ± 5.34	70.51% ± 2.05	40.19% ± 2.09
	Sofa	TV/monitor		
Adv. Baseline	34.40% ± 28.58	39.80% ± 8.13		
Adv. Semi-sup.	35.00% ± 29.45	18.20% ± 12.51		
Adv. Full	82.20% ± 0.75	64.60% ± 2.50		
DeepLab Baseline	34.95% ± 28.67	43.72% ± 9.62		
DeepLab CowMix	39.51% ± 32.95	63.18% ± 1.10		
DeepLab Full	81.98% ± 0.13	68.15% ± 1.80		
U-net Baseline	17.64% ± 16.75	29.58% ± 7.32		
U-net CowMix	33.16% ± 27.70	46.93% ± 6.07		
U-net Full	75.06% ± 1.67	70.86% ± 1.11		

Table 6: Per-class performance on augmented PASCAL VOC dataset, 100 supervised samples